Distribution Agreement

In presenting this thesis as a partial fulfillment of the requirements for a degree from Emory University, I hereby grant to Emory University and its agents the non-exclusive license to archive, make accessible, and display my thesis in whole or in part in all forms of media, now or hereafter now, including display on the World Wide Web. I understand that I may select some access restrictions as part of the online submission of this thesis. I retain all ownership rights to the copyright of the thesis. I also retain the right to use in future works (such as articles or books) all or part of this thesis.

Kayoko Fong April 4, 2019

Striatal ΔFosB gene silencing reduces abnormal involuntary movements induced by L-DOPA in hemiparkinsonian rats

by

Kayoko Fong

Dr. Stella Papa
Adviser

Department of Human Health

Dr. Stella Papa

Adviser

Dr. Michelle Lampl

Committee Member

Dr. Ellen Hess

Committee Member

2019

Striatal ΔFosB gene silencing reduces abnormal involuntary movements induced by L-DOPA in hemiparkinsonian rats

By

Kayoko Fong

Dr. Stella Papa

Adviser

An abstract of
a thesis submitted to the Faculty of Emory College of Arts and Sciences
of Emory University in partial fulfillment
of the requirements of the degree of
Bachelor of Arts with Honors

Human Health

2019

Abstract

Striatal ΔFosB gene silencing reduces abnormal involuntary movements induced by L-DOPA in hemiparkinsonian rats

By Kayoko Fong

Over the course of long-term treatment of Parkinson's Disease (PD) with L-DOPA, a condition called L-DOPA-induced dyskinesias (LID) can emerge, severely affecting the quality of life of PD patients. LID manifests as abnormal involuntary movements (AIMs) and while its pathogenesis is largely unknown, its development has been linked to transcription factors, including ΔFosB, a truncated form of FosB. Using a hemiparkinsonian 6-hydroxydopamine (6-OHDA) rat model, we investigated whether inhibiting ΔFosB expression with viral vector gene transfer would reduce and/or delay the onset of AIMs. We found evidence of the former (i.e. reduced AIMs scores), but not the latter, and these results, attributed to the role of ΔFosB, were further supported by Western blotting analysis, showing less expression of ΔFosB. Furthermore, the total and peak rotation numbers as well as other behavioral tests, i.e., cylinder and stepping, did not differ significantly between the ΔFosB and control groups, indicating similar antiparkinsonian effects of L-DOPA. These results reinforce ΔFosB's importance in the development of AIMs and support the potential for ΔFosB gene silencing as a future therapeutic for LID.

Striatal ΔFosB gene silencing reduces abnormal involuntary movements induced by L-DOPA in hemiparkinsonian rats

By

Kayoko Fong

Dr. Stella Papa

Adviser

A thesis submitted to the Faculty of Emory College of Arts and Sciences
of Emory University in partial fulfillment
of the requirements of the degree of
Bachelor of Arts with Honors

Human Health

2019

Acknowledgements

I would like to thank Dr. Stella Papa for her guidance and faith, from accepting me into her lab to letting me pursue this research question. This study would not have been possible without Dr. Goichi Bekku, whose patience and help during each phase of this project was invaluable. I am grateful to Dr. Freeman, for her honest and practical advice in leading me through the tumultuous process of writing and defending an honors thesis. I want to thank Dr. Mouradian and her lab for constructing and providing the viral vectors as well as executing the western blot analysis, which were critical components of the experiment. Additionally, I want to acknowledge the time and consideration of my two other committee members, Dr. Ellen Hess and Dr. Michelle Lampl.

Finally, for my family:

To Mom and Dad, for not flinching and trusting my judgment when I decided to conduct research in animals with deadly zoonotic diseases. You both have empowered me to think critically about the world around me, prompting me to discover who I am as well as who I hope to become. I am unable to articulate how deeply grateful I am to be your daughter.
To Gen Gen, for being an inspirational example of tenacity and hard work. You are my feminist icon.
To Yeh Yeh, for loving and understanding me in a way no one else could.
To Grandpa, for recognizing my love of science early on and for becoming the face of all PD patients to whom this research is ultimately dedicated.

Table of Contents

List of Figures

Introduction

Parkinson's Disease (PD) is a neurodegenerative disease, characterized by a progressive denervation of dopamine-producing neurons in the substantia nigra pars compacta. Worldwide, PD patients are an estimated 2-3% of the population age 65 or older. However, like many neurodegenerative diseases, the prevalence of PD increases with age (Poewe et al., 2017), so the number of PD patients from 2005 is expected to double by 2030, due to increasing life expectancy and the demographic transitions of aging nations (Dorsey et al., 2007).

Outside of a small minority, about 10%, of PD cases that are hereditary, caused by inherited mutations of genes that encode defective proteins (Klein and Westenberger, 2012), most PD cases are idiopathic. Idiopathic refers to the fact that the cause of PD largely remains elusive. Idiopathic PD is regarded as multifactorial, with causes resulting from the interaction between environmental factors (e.g. age, exposure to chemicals, diet, and lifestyle) as well as genetics (Schulte and Gasser, 2011). With idiopathic PD, it is believed that a patient's genetic predisposition to PD is influenced by his or her lifetime exposure to environmental factors. Unfortunately, since the cause of PD is not well-delineated and PD is a neurodegenerative disorder, all current treatments are symptomatic and cannot alter the progression of and inevitable disability associated with PD.

For patients with PD, L-DOPA remains the "gold standard" treatment (Poewe et al., 2010), replacing dopamine (DA) after being catalyzed by an aromatic L-amino acid decarboxylase. In order to promote the accumulation of dopamine in the brain, L-DOPA is generally paired with benserazide, a peripheral decarboxylase inhibitor. In its capacity as a decarboxylase inhibitor, benserazide prevents the premature conversion of L-DOPA to dopamine from occurring before entering the brain.

In the early years of treatment, L-DOPA, in combination with benserazide, effectively alleviates cardinal motor symptoms like bradykinesia, rigidity, postural instability, and resting tremor. However, chronic L-DOPA therapy is associated with several side effects including motor complications. The most severe and disabling of these is L-DOPA-induced dyskinesias (LID), which are repetitive and senseless movements. Key risk factors for LID are age, including young age of PD onset and with risk increasing with age, high dose of L-DOPA, duration of L-DOPA exposure, and degree of nigrostriatal dopaminergic denervation, indicative of the severity of the patient's PD (Thanvi et al., 2007).

LID affects an estimated 40-50% of patients after five years of treatment (Ahlskog & Muenter, 2001; Parkinson Study, G., 2004). After 15 years, one study found that 94% of PD patients developed LID (Hely et al., 2005), suggesting that LID will manifest in the majority of those who are chronically treated with L-DOPA. Once LID emerges, its severity will increase over time (Lee, 2001), presenting a treatment dilemma of whether to lessen the total daily dose of L-DOPA, reducing the severity of "peak dose dyskinesia," at the expense of lessening L-DOPA's antiparkinsonian effects (Lee, 2001; Manson et al., 2012).

The treatment of LID has been challenging and has largely relied on an empiric basis, particularly because the underlying mechanisms of LID have not been established. Current treatment approaches for LID include amantadine, a former influenza prophylactic discovered to ameliorate dyskinesias (Sharma et al., 2018) and deep brain stimulation targeting the subthalamic nucleus to relieve most motor symptoms in PD including LID (Pahwa et al., 2006). As a noncompetitive antagonist of the NMDA receptor (NMDAR), amantadine's antidyskinetic effects may result from blocking the upregulated excitatory input of glutamate, which is a neurotransmitter that acts as an agonist at the NMDAR (Paquette et al., 2008). While these

treatments help to manage dyskinesias, our current knowledge of how dopaminergic drugs act in the basal ganglia and impair motor function over time has limited the development of specific therapies. Our experiment targets a chronic transcription factor, ΔFosB, in an effort to demonstrate its primary link to the pathogenetic mechanism of LID, and lead to development of more specific treatments.

Previous studies have shown the association of ΔFosB with the emergence of LID in animal models of PD (Tekumalla et al., 2001; Du, et al., 2015; Patterson et al., 2016). In rats, transgenically overexpressed ΔFosB, without being induced by chronic L-DOPA treatment, produced LID comparable to LID resulting from chronic L-DOPA treatment (Cao et al, 2010). In rats, abnormal involuntary movements (AIMs) are the equivalent of primate-human LID and thus, AIMs are used as a proxy for LID in rat models of PD (Lundblad et al., 2002). These studies correlate an increase in striatal ΔFosB expression with long term L-DOPA treatment or the overexpression of ΔFosB itself with the appearance of LID. A direct relationship between the amount of ΔFosB and severity of dyskinesias has been observed in both rats (Bastide et al., 2014) and non-human primates, NHP (Berton et al., 2009). However, whether ΔFosB plays a primary role in LID mechanisms has not been determined.

ΔFosB is part of a larger group of transcription factors, “chronic FRAs” (Fos-related antigens) and as with other chronic FRAs that can increase their activity in the brain due to chronic perturbations, ΔFosB’s activity similarly increases due to the overstimulation of dopamine receptors during chronic L-DOPA therapy. The sensitized response that follows overstimulation prompts increased ΔFosB activity, starting with the dysregulation of D1 DA receptor (D1R) signaling in the striatum that precedes the onset of LID (Westin et al., 2007; Darmopil et al., 2009). D1R, coupled with Gαolf, stimulates the cAMP/PKA cascade, first by

activating adenylyl cyclase type 5 and in turn, catalyzing the production of cyclic AMP (cAMP) from ATP. cAMP binds to the regulatory subunits of protein kinase A (PKA), activating the catalytic subunits of PKA, which then dissociate from the regulatory subunits. In its active state, PKA is able to phosphorylate many downstream targets like DARPP-32 (Alcacer et al., 2012; Goto, 2017). The activation of DARPP32 leads to the phosphorylation of ERK (Pavón et al., 2006; Feyder et al., 2011) as DARPP32 inhibits the striatal-enriched protein tyrosine phosphatase (STEP), which deactivates ERK (Valjent et al., 2005). Thus, the phosphorylation of DARPP32 links the cAMP and ERK1/2/MAP pathways (Santini et al., 2010; Fisone & Bezard, 2011; Fiorentini et al., 2013; Heumann et al., 2014). Heightened ERK1/2 signaling has important implications for LID development, leading to increased cAMP response element binding (CREB) phosphorylation (Calabresi et al., 2008). After phosphorylation, active CREB binds to the CREB-binding protein (CBP) at the CREB-binding element in the 5' promoter region, resulting in increased transcription. Thus, greater ERK1/2 signaling is capable of upregulating many LID related transcription factors, like **Δ**FosB.

Notably, ΔFosB has extended induction kinetics, heightening its effects as a chronic FRA, and atypical stability, allowing those increased effects to last longer (Andersson et al., 2003; McClung et al., 2004; Ulery et al., 2006). ΔFosB plays a crucial role in facilitating intracellular signaling and transcriptional changes in the striatum, beginning with the heterodimer it forms with JunD, another transcriptional protein (Hope et al., 1994; Chen et al., 1997; Hiroi et al., 1998). The ΔFosB and JunD heterodimer then binds to the AP-1 site in 5' promoter regions in a variety of downstream target genes. These complexes, called chronic activator protein-1 (AP-1), regulate late response genes, by promoting or repressing transcription, and they may cause stable functional changes that potentiate over the course of L-

DOPA treatment (Hope et al., 1994; Jorissen et al., 2007). These mechanisms suggest that ΔFosB may be a messenger capable of inducing genes that participate in a cascade of molecular reactions leading to cellular responses to L-DOPA and LID development.

Given the critical role of ΔFosB and its correlation with LID onset, this project employed gene silencing, a method that has gained traction as potential therapeutic strategy in other neurodegenerative diseases (Manczak and Reddy, 2013) in addition to PD. The focus of these previous studies was on RNA interference with the expression of relevant genes, mediated by siRNA-expressing viral vectors. Rather than siRNA, this study used short hairpin RNA (shRNA), which still selectively interferes with RNA like siRNA, but is also capable of creating stable changes over a longer period of time (Rao et al., 2009).

In previous PD models testing the use of gene silencing, there have not yet been any attempts made to silence ΔFosB. An earlier study silencing ΔFosB expression by Chen and colleagues (2006) utilized an antisense knockdown of ΔFosB to showing reduced LID in rats (Chen et al., 2006). Although effective in silencing ΔFosB, there are some critical drawbacks of using an antisense oligonucleotide as a potential therapeutic. These drawbacks include its unknown toxicity in humans and unintended sequence and structural changes that occur *in vivo*, known as off-target effects (Rayburn and Zhang, 2008). Conversely, ΔFosB expression was silenced in this study using a recombinant adeno-associated virus (rAAV), which is nonpathogenic and, in clinical trials for PD, has shown to be safe while demonstrating effective transduction (Bartus et al., 2014).

Thus, the viral vector, rAAV-ΔFosB shRNA-GFP, silencing ΔFosB expression allowed for a direct investigation between its relationship to LID generation. A confirmation of ΔFosB's leading role in LID development will encourage further study of the mechanisms that

ΔFosB directs, ultimately causing the appearance of LID. While viral vector gene transfer was successfully employed to reproduce abnormal involuntary movements by overexpressing ΔFosB in rats (Cao et al., 2010), we silenced ΔFosB expression using shRNA in rats to determine causality of this transcription factor in LID development. Further studies will be necessary to assess the potential of this strategy as a future gene therapy for LID.

Materials and Methods

rAAV-Viral Vector Construction

As a novel strategy to silence ΔFosB, a new viral vector had to be constructed, initial tests were run in order to determine the optimal shRNA sequence to interfere with ΔFosB gene transcription. Finally, the serotype 5 of the rAAV virus was selected because it transduces in a large number of cells in the striatum, the injection site in this study (Paterna et al., 2004).

The viral vectors were constructed by the Mouradian laboratory at Rutgers University.

Ten different sequences of shRNA targeted to the rat mRNA ΔFosB were synthesized, purified with HPLC, and tested for specificity against the ΔFosB mRNA. The latter was accomplished by transfecting rat PC12 cells with vectors containing the sequences and determining endogenous levels of ΔFosB with Western blotting. The most effective of these sequences were selected and then, along with the scrambled shRNA, were inserted into the pAAV-MCS plasmid with promoter CAG, at *Bgl*II and *Xba*I sites, respectively. The plasmids, pAAV-ΔFosB shRNA and control, were then co-transfected with plasmid pHelper and Pack2/1 to HEK293T cells, producing the rAAV viral vector, with purified copies confirmed with PCR.

6-OHDA Rat Model

Each rat (Sprague-Dawley; n=13) was anesthetized with ketamine (90 mg/kg, i.p.) and xylazine (6.5 mg/kg, i.p.) before its head was shaved, its skin cut at a length of 15 mm and its skull, exposed. The rat was placed on the stereotaxic frame, the incisor teeth fixed with the nose bar set at -4.5 mm and ear bar horizontally. The rat was given an analgesic treatment postoperatively. The microsyringe holder was connected to the bar of the stereotaxic frame, with the interaural line used as zero. The injection point was determined according to the following stereotaxic coordinates for the medial forebrain bundle: A, 4.0 mm; L, 1.3 mm from the middle of the interaural line; and V, 8.4 mm from surface of the skull. A hole was then drilled on the skull at the coordinates' point. The microsyringe, tubing and needle system was filled with 6-OHDA solution and the needle was lowered to target area in the brain. 6-OHDA was injected using a microinfusion pump (at a rate of 0.5 uL/min) delivering 4 uL. The needle was slowly withdrawn at 1 mm/min to allow 6-OHDA to diffuse until the needle was completely removed. The skin was sutured and atipamezole (0.5 mg/kg i.p.) was injected to reverse xylazine effects.

Preparation of 6-OHDA Solution

6-OHDA was dissolved to 2 mg/mL in 0.02% ascorbic acid. Ascorbic acid was prepared with a ratio of 20 mg dissolved in 100 mL of saline.

Viral Injection

Either rAAV-ΔFosB shRNA-GFP (n=7) or control, rAAV-scrambled shRNA-GFP (n=6) was injected to rats into the striatum ipsilateral to the nigrostriatal lesion. The virus solution was injected with a Hamilton microsyringe at 0.5 uL/min, and according to the striatum stereotaxic coordinates: at A, 8.4 mm; L, 4.4 mm from the middle of the interaural line; and V, 6.2 mm and 5.2 mm from surface of the skull.

Apomorphine test

Three weeks after the 6-OHDA and viral injections, a rotational behavioral test was carried out using a subthreshold dose of the DA agonist, apomorphine (0.05 mg/kg, s.c.). According to Yuan et al. (2005), three weeks is the amount of time before a full dopaminergic lesion, defined as < 1% DA left in striatum, is created after a 6-OHDA injection in the medial forebrain bundle. The apomorphine test determined which subjects were the successful models, with rotational behavior >7r/min, indicating a complete dopaminergic lesion. Results from the apomorphine test are not included in the figures section, but were applied as part of the screening process, prompting the removal of subjects that did not have complete lesions before L-DOPA treatment and behavioral tests. Apomorphine was dissolved to 2 mg/mL in 0.2% ascorbic acid.

Behavioral tests

Following surgery, rats from both groups were assigned new numbers, but these were not known to researchers who scored AIMs and conducted behavioral tests like the cylinder and stepping (blinded scoring). Two researchers independently scored by direct examination.

Behavioral tests began two weeks following the apomorphine test and 5 weeks following surgery, allowing either the control or ΔFosB gene knockdown virus to be fully transduced in the striatum.

Scoring AIMs

AIMs were measured using three categories of dyskinetic behavior, classified as axial dystonia, limb dyskinesias, and masticatory (orolingual) dyskinesias, modified from previous scales (Lee et al., 2000; Cenci and Lundblad, 2007). Lundblad et al. (2002) concluded that only the three aforementioned categories of AIMs, collectively referred to as ALO (axial, limb, and orofacial), align well with the expression of LID in primates and humans, including peak-dose dyskinesia,

affecting upper trunk, limbs, and orofacial muscles (Pandey and Srivanitchapoom, 2017). The excluded category, locomotive AIMs, which are basically contralateral rotations counted by the rotometer were not included as a category of LID in hemiparkinsonian rats (Sgroi et al., 2014). Within each category, the presence of each behavior was determined on a scale from 0 (absent) to 4 (severe) every 15 minutes over a 90 minute period. The total of each category at a given time point was used to calculate an overall AIMs score. These behavioral tests were conducted on day 1, day 4, day 8, day 11, day 15, and day 18 of the daily administrations of L-DOPA. Concurrent with these tests was the automatic counting of the subjects' rotations in clockwise and counterclockwise directions by a rotometer and its associated software. Total rotation is the number of contralateral turns (clockwise) over the 90 minute interval, while peak rotation refers to the maximum number of contralateral turns within any five minute interval during the 90 minute time frame.

Cylinder test

The animals were individually placed in a 20-cm-diameter glass cylinder, in which they moved freely and explored. The weight-shifting movements of the forepaws in contact with the wall of the glass cylinder are scored, testing limb use asymmetry (Mabandla et al., 2015). A total of 20 touches using either the left or right forepaw with the wall of the cylinder was noted for each animal, and the data was presented as the use of the right (impaired) paw as a percentage of total touches. In normal controls with equal use of the two paws, the score is thus 50%. Cylinder tests were conducted both before and 30 minutes after L-DOPA injection at both baseline and day 19.

Stepping test

The rat was held by the experimenter with one hand fixing the hindlimbs and slightly raising the hind part above the surface. The other hand fixed the forelimb not being monitored. Time was

measured until the rat initiated movement with the forelimb not fixed by the experimenter, using 180 seconds as the break-off point. Stepping tests were conducted both before and 30 minutes after L-DOPA injection at both baseline and day 19.

"Stepping time" was measured from initiation of movement until the rat travelled 0.9 m and the sequence of testing was right paw testing followed by left paw testing. The "stepping test" is a measure of bradykinesia (Fang et al., 2006) and so the longer amount of time it takes to initiate movement, the more the subject is considered to be parkinsonian.

Adjusting steps

The rat was held in the same position as described above with one paw touching the table, and then moved slowly sideways (5 seconds for 0.9 m) by the experimenter. The number of adjusting steps was counted for both paws in the backhand and forehand directions of movement. The sequence of testing was right paw forehand and backhand adjusting stepping, followed by left paw forehand and backhand directions. Adjusting steps tests forelimb akinesia in both forehand and backhand directions (Olsson et al., 1995). Forelimb akinesia in the hemiparkinsonian rat model is comparable to limb akinesia and gait problems that manifest in human PD patients. Akinesia affects PD patients' ability to initiate and execute spontaneous movement, including learned patterns of movement in abnormal gait (Berardelli et al., 2001).

Chronic L-DOPA treatment

Each rat was administered one daily dose of L-DOPA plus benserazide (12/12 mg/kg, i.p.) for 18 days. Subsequently, all future references to L-DOPA refer to a mixture of L-DOPA and benserazide at the dosage of 12 mg/kg.

The dosage regimen follows established treatment models of producing AIMs in 6-OHDA rats, which vary from 6/6 mg/kg to 15/15 mg/kg (Lee et al., 2000; Cenci and Lundblad, 2007). 12/12

mg/kg was selected as it is at the upper end of this range, providing a sufficiently dyskinetic dose of L-DOPA for testing the hypothesis that ΔFosB gene knockdown is protective of AIMs.

Immunohistochemistry

Rats were sacrificed while deeply anesthetized within 12 hours after last L-DOPA injection on day 19 and prepared as outlined in Cao et al. (2010) in the Mouradian laboratory at Rutgers University. Brain blocks from the striatum were alternately divided for either postfixation with 4% PFA for immunohistochemistry, or stored at −80°C for Western blotting.

Coronal sections (30-µm) were cut serially using a freezing microtome, and free-floating sections were washed in PBS containing 0.05% Triton X-100 (PBS-T) and then incubated for 30 min with 0.3% H_2O_2 to quench endogenous peroxidase activity. Sections were soaked with blocking agents and then incubated with primary antibodies dissolved in dilution reagent at 4°C for 24 h. Normal Goat Serum Blocking Solution (S-1000, Vector Laboratories, Burlingame, CA, USA) was used for blocking. A mouse monoclonal antibody against GFP (1:100, sc-9996, Santa Cruz Biotechnology, Dallas, TX, USA) was used as the primary antibody. Alexa Fluor® 488 goat anti-mouse IgG (H + L) antibody (A-11001, ThermoFisher Scientific, Waltham, MA, USA) was used as the secondary antibodies. Images were obtained using ECLIPSE E800 (Nikon, Tokyo, Japan). For cell counting, 10 images were obtained using a digital camera connected to a microscope (40× objective) in each animal, and GFP-positive cells were counted, respectively.

Sections (30-µm thickness) of the post-fixed blocks of the brain were washed with Phosphate Buffered Saline (PBS) and before incubation with hydrogen peroxide (H2O2) for 10 min. Following rinsing with additional PBS, sections were placed in 10% normal goat serum (NGS)/1% bovine serum albumin/PBS for 30 min before being incubated with the GFP

antibody: rabbit polyclonal anti-GFP (AB3080, 1:200 dilution, Millipore, Chemicon). After incubation, sections were processed with a Vectastain ABC kit (Vector Laboratories) for 1 hour. The number of GFP positive cells were counted using bounded areas in the posterior-lateral striatal areas that are related to sensorimotor regions. The limits of these areas were determined using the Olympus CAST 2.0 system (Olympus Denmark A/S) from six equal sized sections that collectively covered the majority of the striatal volume, from the rostral tip to the level of globus pallidus. With these six regions, the Olympus system produced a select number of uniform fields of vision throughout the respective region. The total number of cells was estimated based on the field sampled by the program.

GFP positive cells were counted because GFP was a tagging protein used in both viral vectors. Thus, the finding of GFP positive cells confirmed the successful transduction of the viral vector and the comparable number of GFP positive cells in both types indicated a similar transduction following the injection of either viral vector.

Immunofluorescence

Sections were incubated in 5% normal donkey serum in PBS for 10 minutes before being incubated overnight at 4°C in a GFP antibody solution. Sections were washed in PBS before incubation in FITC-conjugated donkey anti-rabbit IgG (1:200 dilution, Jackson Laboratories). Before imaging, sections were washed in PBS and mounted on slides. After coverslipping, the slides were viewed under a fluorescent microscope (ECLIPSE E800, Nikon).

Western blotting

The left and right striata were dissected from frozen brain blocks. Both striata were homogenized in a lysis buffer with protease inhibitor and centrifuged. The protein content of supernatants was

evaluated with a BCA protein assay kit. Using SDS-PAGE (10% gels), 10 μg of protein/well were separated and then placed onto polyvinylidene fluoride (PVDF) membranes. To prevent nonspecific binding, these membranes were blocked in Tris-Buffered Saline with Tween (TBS-T) and 5% non-fat dry milk (NDM) before being incubated overnight at 4°C with the primary antibody, diluted at 1:1000 for anti-FosB/ΔFosB. Membranes were washed 4 times for 15 min with TBS-T before incubating for 1 hour at room temperature with horseradish peroxidase-conjugated anti-rabbit antibody (1:2000 dilution, Santa Cruz Biotechnology) in TBS-T. Three additional washes in TBS for 10 minutes followed each antiserum application. ECL allowed for the separation of FosB and ΔFosB bands and actin was used as a loading control.

Statistical Analysis

Behavioral data from the control and rAAV-ΔFosB shRNA groups were processed using two-way ANOVA for repeated measures followed by Fisher's least significant difference (LSD). For AIMs, ANOVA for repeated measures compared the scores within each group across multiple time points (days 1, 4, 8, 11, 15, and 18). The results from the stepping and cylinder tests also underwent two-way ANOVA for repeated measures, but with two time points, baseline and day 19. The statistical analysis including both within and between subjects was also run with the use of SPSS.

Results

Reduction of AIMs following ΔFosB Gene Knockdown

Figure 1 clearly illustrates that ΔFosB knockdown significantly reduces AIMs, at $p < 0.05$, between the rAAV-ΔFosB shRNA-GFP and control groups starting at day 8, when AIMs were robust in the control group. For days 1-4, both groups show increasing AIMs scores, but by day

8, only the control continued to have a greater AIMs score, while the rAAV-ΔFosB group had a lower score. AIMs scores for the rAAV-ΔFosB shRNA-GFP drop further by day 11 before stabilizing between days 15-18. Conversely, AIMs scores of the control group were stable from day 8 to day 15 before sharply increasing on day 18.

Gene Silencing of ΔFosB did not affect antiparkinsonian effects of L-DOPA

The intervention of ΔFosB knockdown using a viral vector is promising not only for the aim of allaying dyskinetic behavior, but also because its actions do not adversely affect the therapeutic, antiparkinsonian effects of L-DOPA. This conclusion is supported by the results from the rotation tests (Figures 2 and 3), which measure the subject's motor response induced by L-DOPA and do not differ significantly between the two groups ($p > 0.05$). More specifically, these antiparkinsonian effects are summarized collectively by the cylinder and stepping tests (Figures 4-9). Taken together, the cylinder and stepping tests demonstrate the improvements of PD symptoms observed in both groups, including limb use asymmetry, bradykinesia, and akinesia, from baseline to the end of chronic L-DOPA treatment.

With ΔFosB not interfering with L-DOPA's function, both groups show no significant difference, $p > 0.05$, at either the baseline or endpoints across both tests, starting as similarly Parkinsonian and finishing with similar improvements on measures of PD symptoms. For the cylinder test (Figure 5), both groups have improved limb use and more closely resemble normal use of both limbs, approaching 50%, where neither the right nor left side is favored. The expected, marked improvements of both groups were observed in decreased initiation time (Figure 7), which is associated with bradykinesia. The same trend was seen with adjusting steps, with comparable number of steps prior and post L-DOPA between the groups, relative to the right or left forepaw. The most dramatic improvement was in the right forepaw after L-DOPA in

both groups, due to the creation of lesion in the left side of the brain, thereby compromising contralateral movement on the right, impaired side.

Efficacy of viral vector-mediated ΔFosB gene silencing

A Western blot, unlike IF, is able to differentiate FosB and ΔFosB expression on the basis of their respective molecular weights, ΔFosB is 33 kDa isoforms and FosB is 46-50 kDa isoforms (Nestler et al., 2001). Figure 10 shows the ΔFosB expression between the control (top) and rAAV-ΔFosB shRNA- GFP (bottom) groups. The striking decreased expression of the gene knockdown group is visible on a Western blot analysis, confirming the effective gene silencing of ΔFosB with the viral vector. Paired with the behavioral results, the biochemical data bolsters the hypothesis and is critical to relating the physiologic data to ΔFosB expression. As predicted, the interference of ΔFosB expression reduced the number of AIMs developed during the course of a chronic L-DOPA treatment.

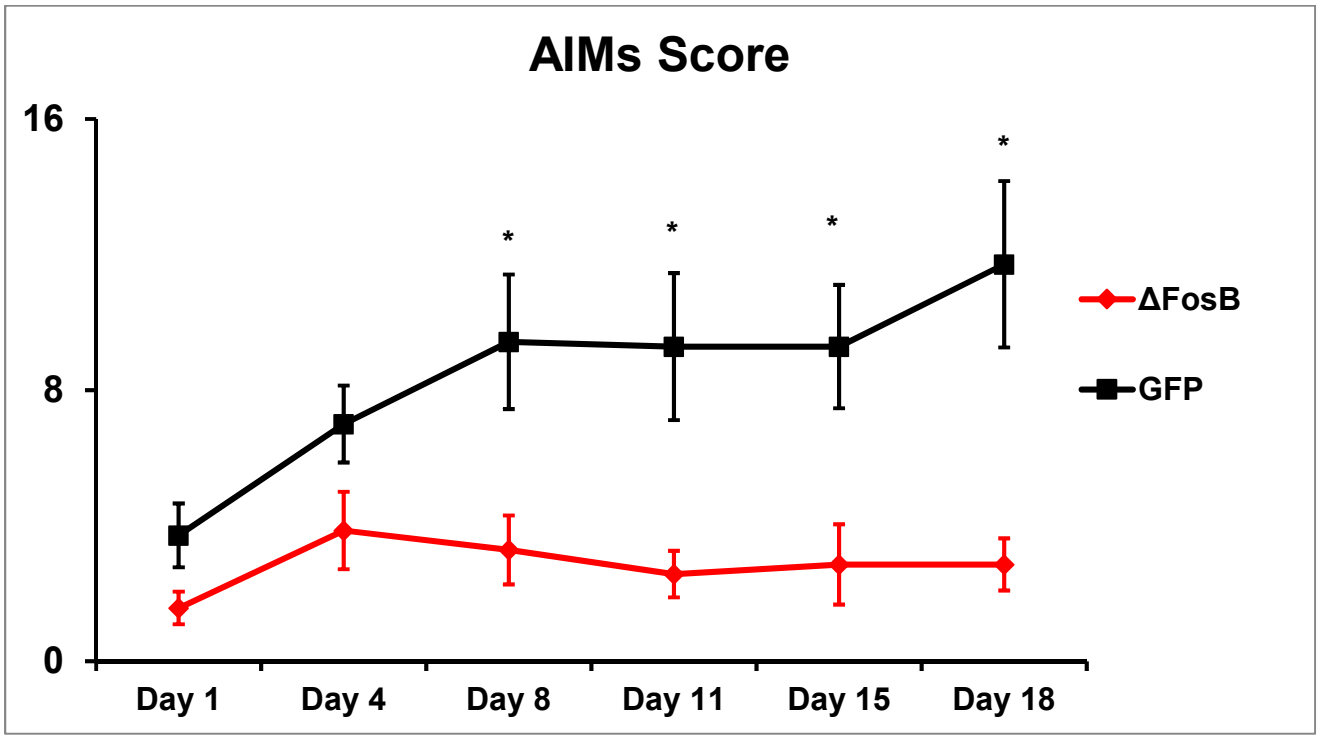

Figure 1. AIMs scores for each group are presented as the mean ± S.E. There is a significant difference in AIMs by day 8 between the control (GFP) and ΔFosB groups, indicated by (*$p < 0.05$).

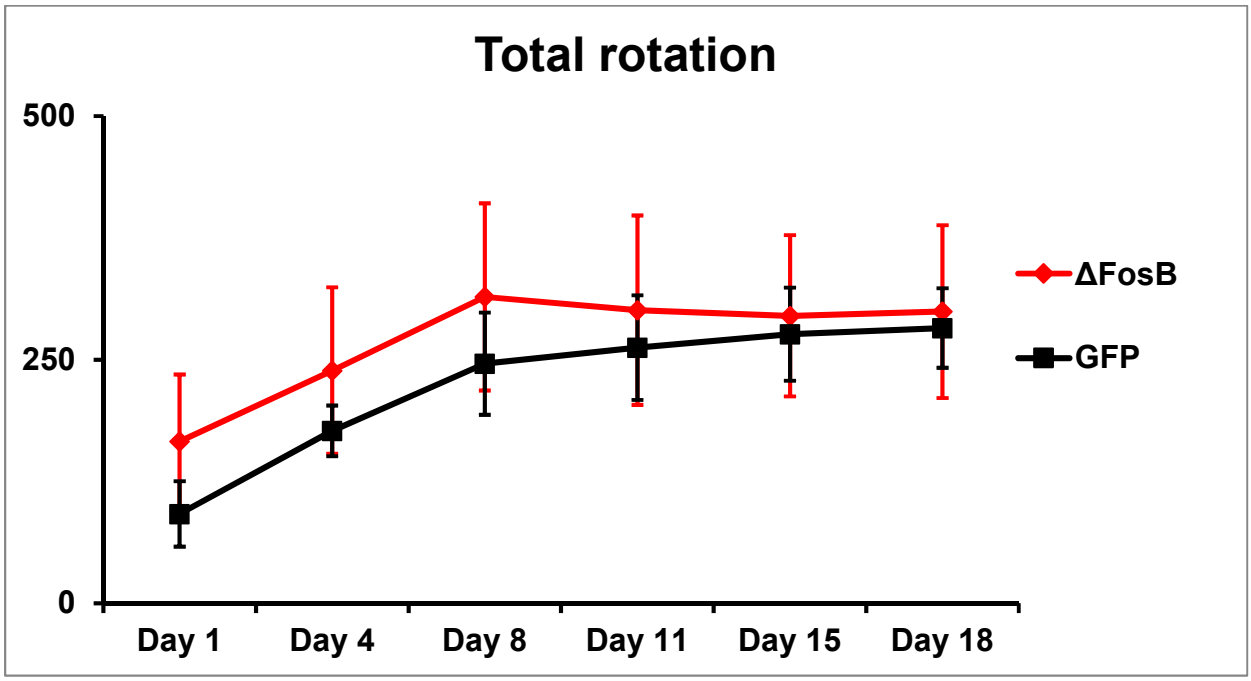

Figure 2. Total rotation measures the motor response induced by L-Dopa (12 mg/kg) plus benserazide (12 mg/kg). There was no significant difference between the groups ($p > 0.05$).

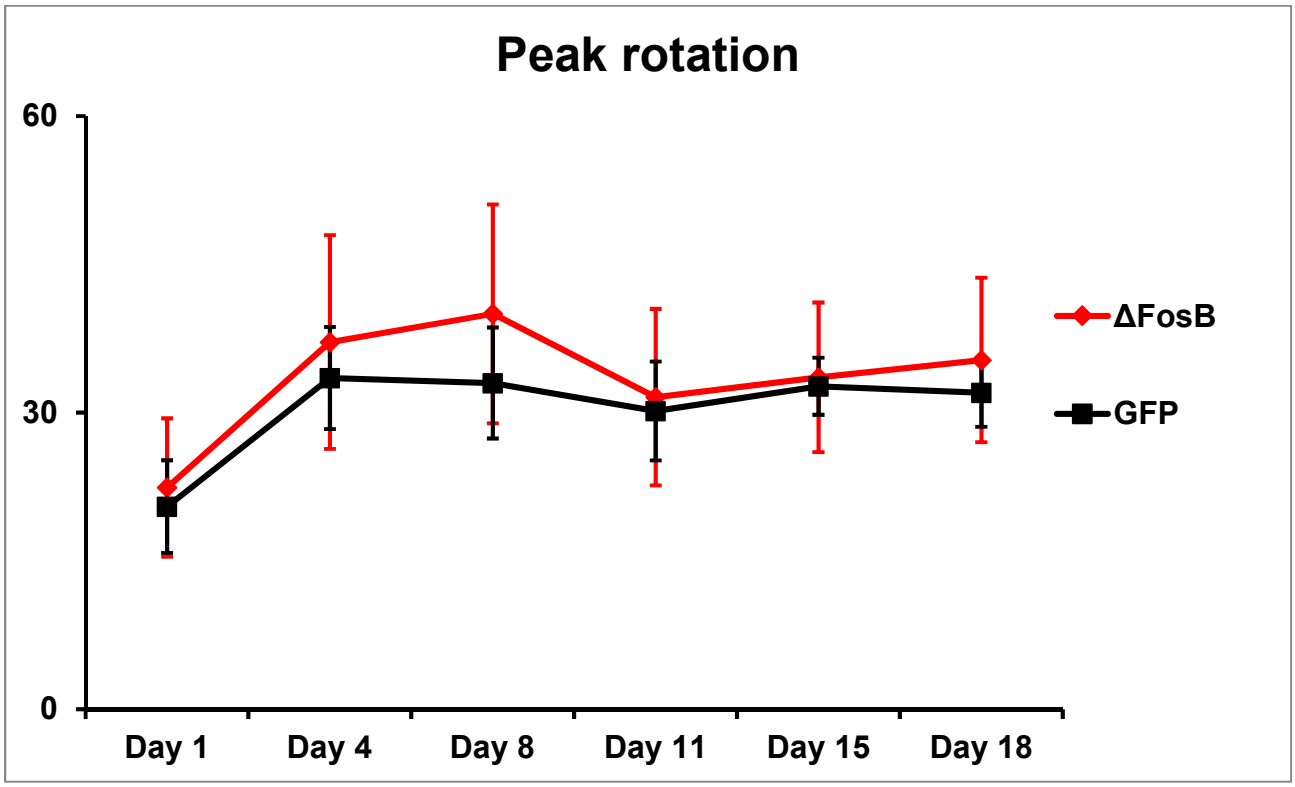

Figure 3. Peak rotation measures the motor response induced by peak dose L-Dopa (12 mg/kg) plus benserazide (12 mg/kg). There was no significant difference between the groups ($p > 0.05$).

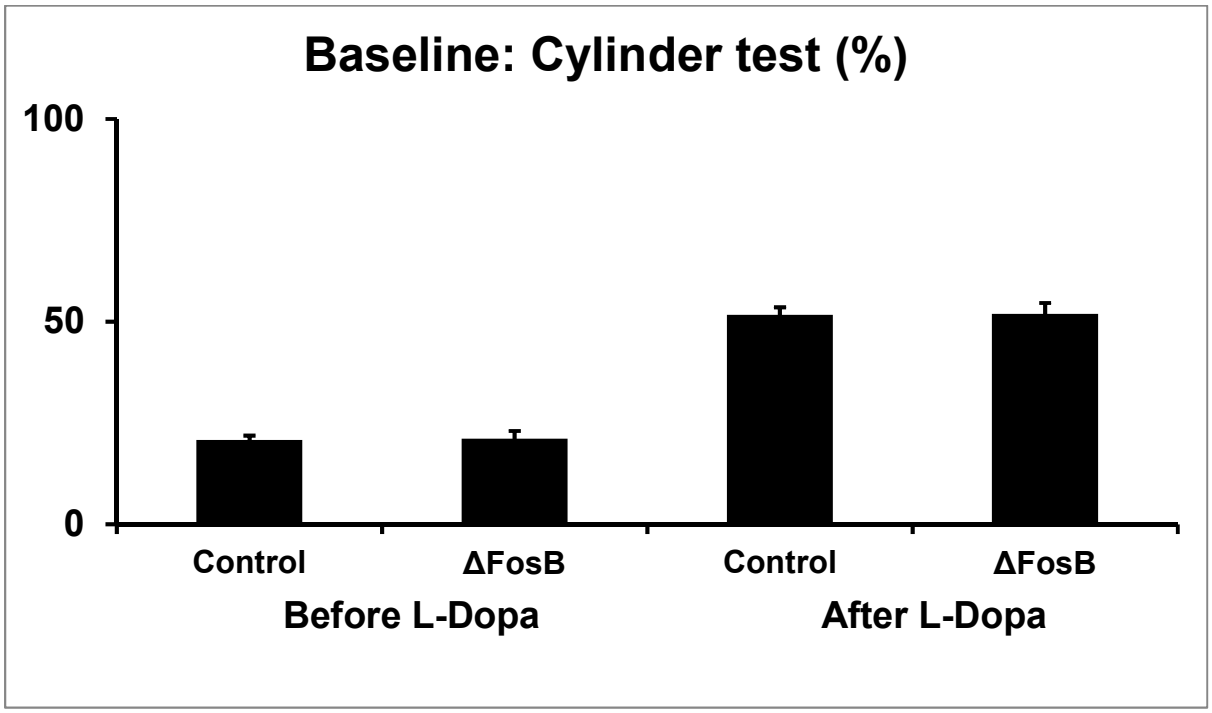

Figure 4. Before and 30 min after L-DOPA injection, cylinder test percentages at baseline are presented as the mean ± S.E. with no significant difference between the groups ($p > 0.05$).

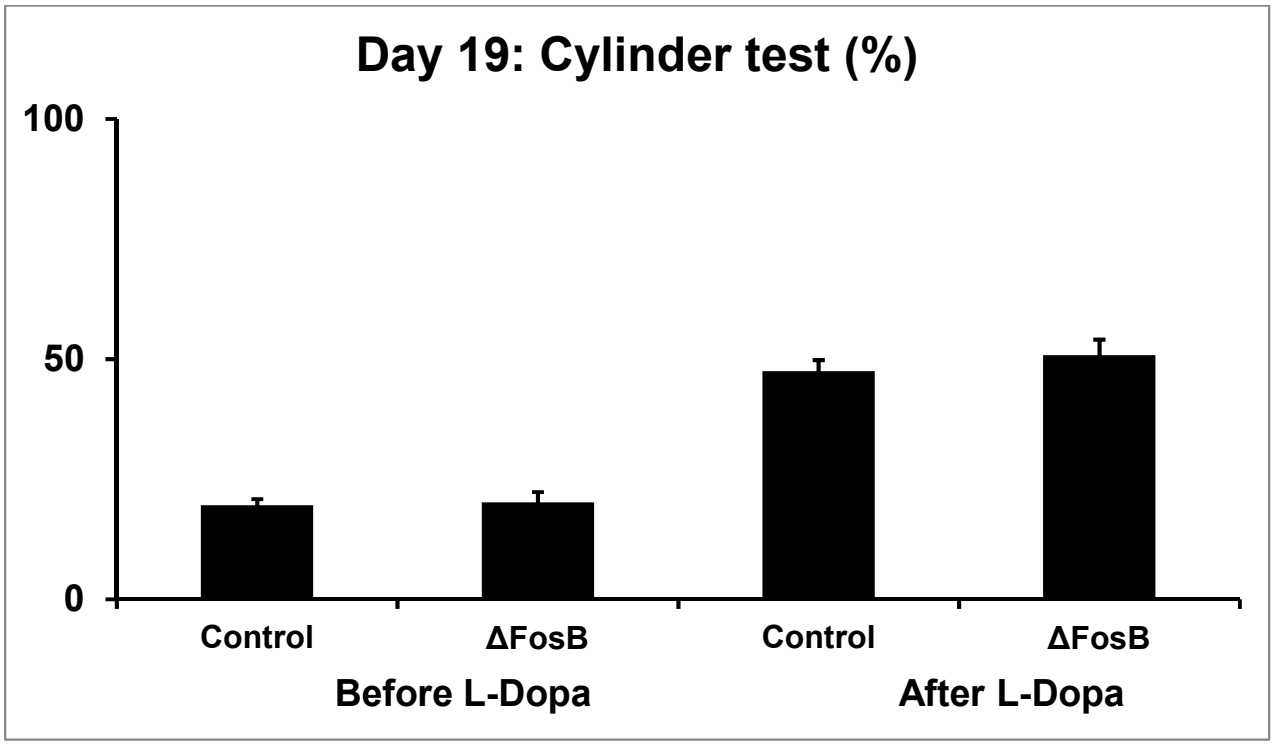

Figure 5. Before and 30 min after L-DOPA injection, cylinder test percentages on day 19 are presented as the mean ± S.E. with no significant difference between the groups ($p > 0.05$).

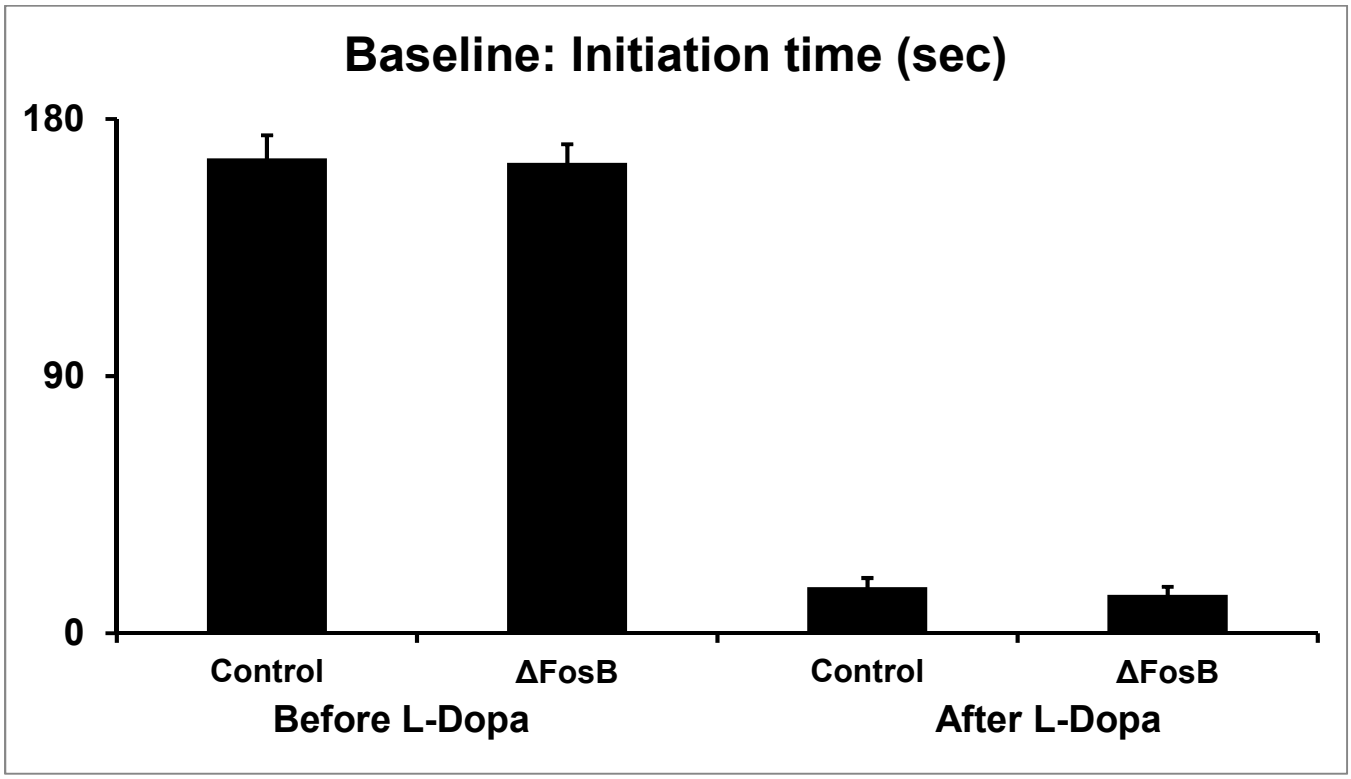

Figure 6. Before and 30 min after L-DOPA injection, initiation times at baseline are presented as the mean ± S.E. with no significant difference between the groups at either time points ($p > 0.05$).

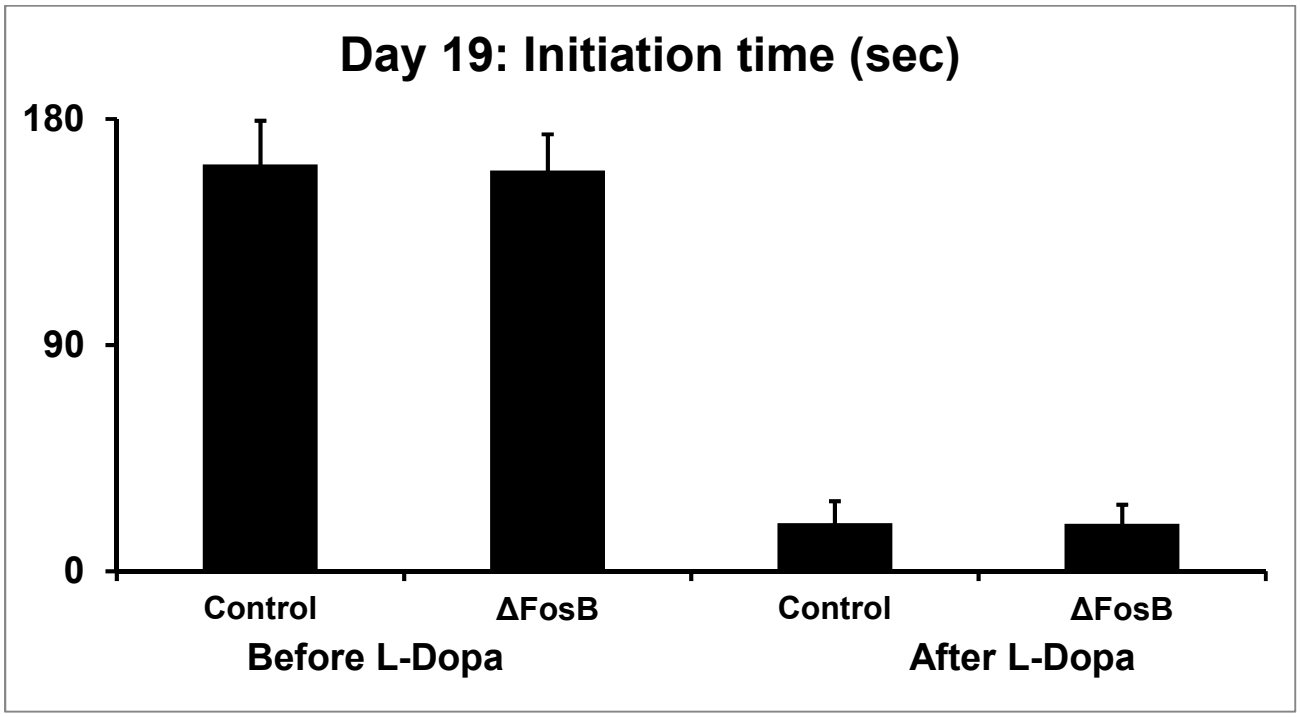

Figure 7. Before and 30 min after L-DOPA injection, initiation times on day 19 are presented as the mean ± S.E. with no significant difference between the groups at either time points ($p > 0.05$).

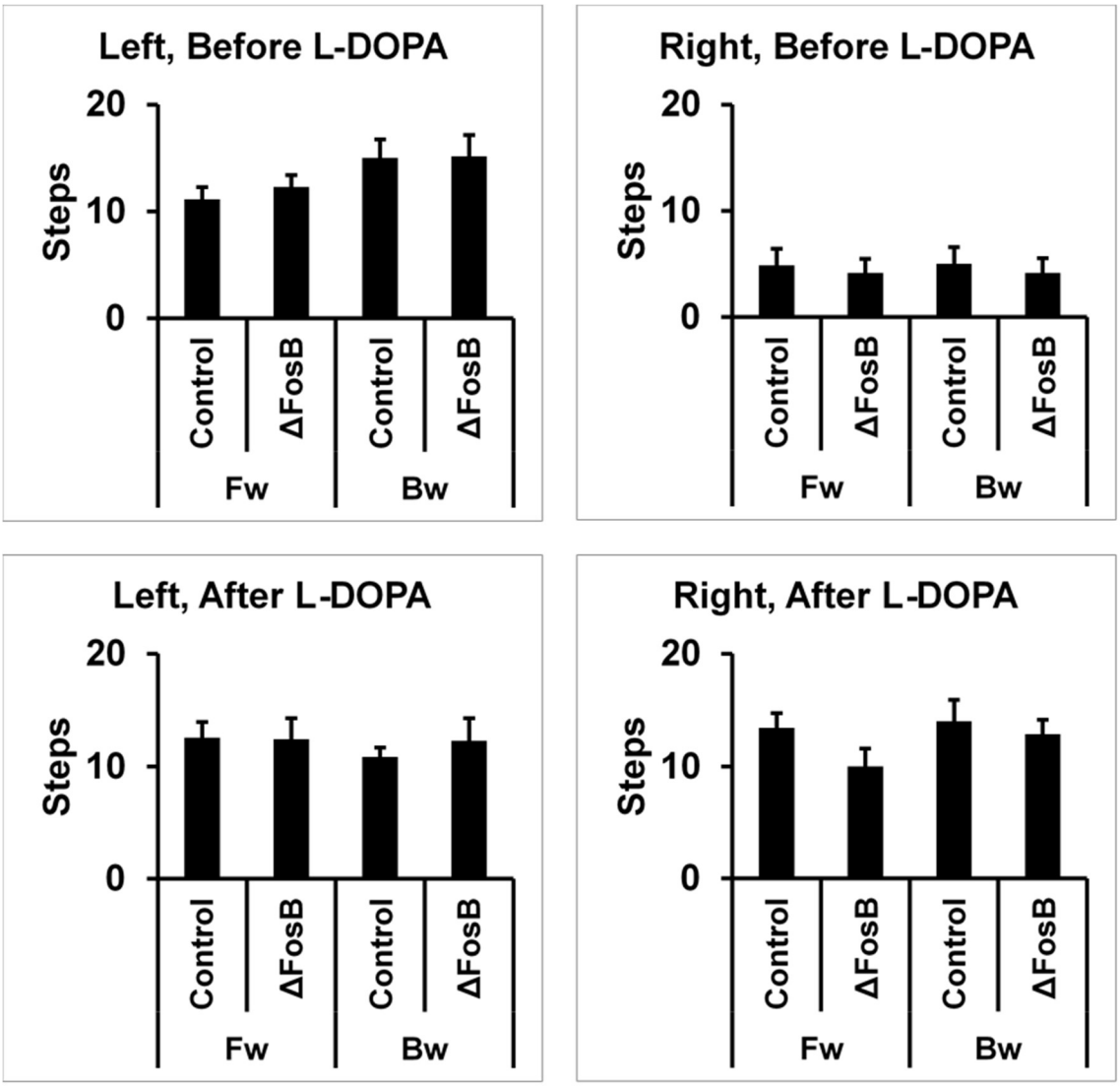

Figure 8. Before and 30 min after L-DOPA injection, there is no significant difference in adjusting steps at baseline between the groups in either the forward or backward direction ($p > 0.05$).

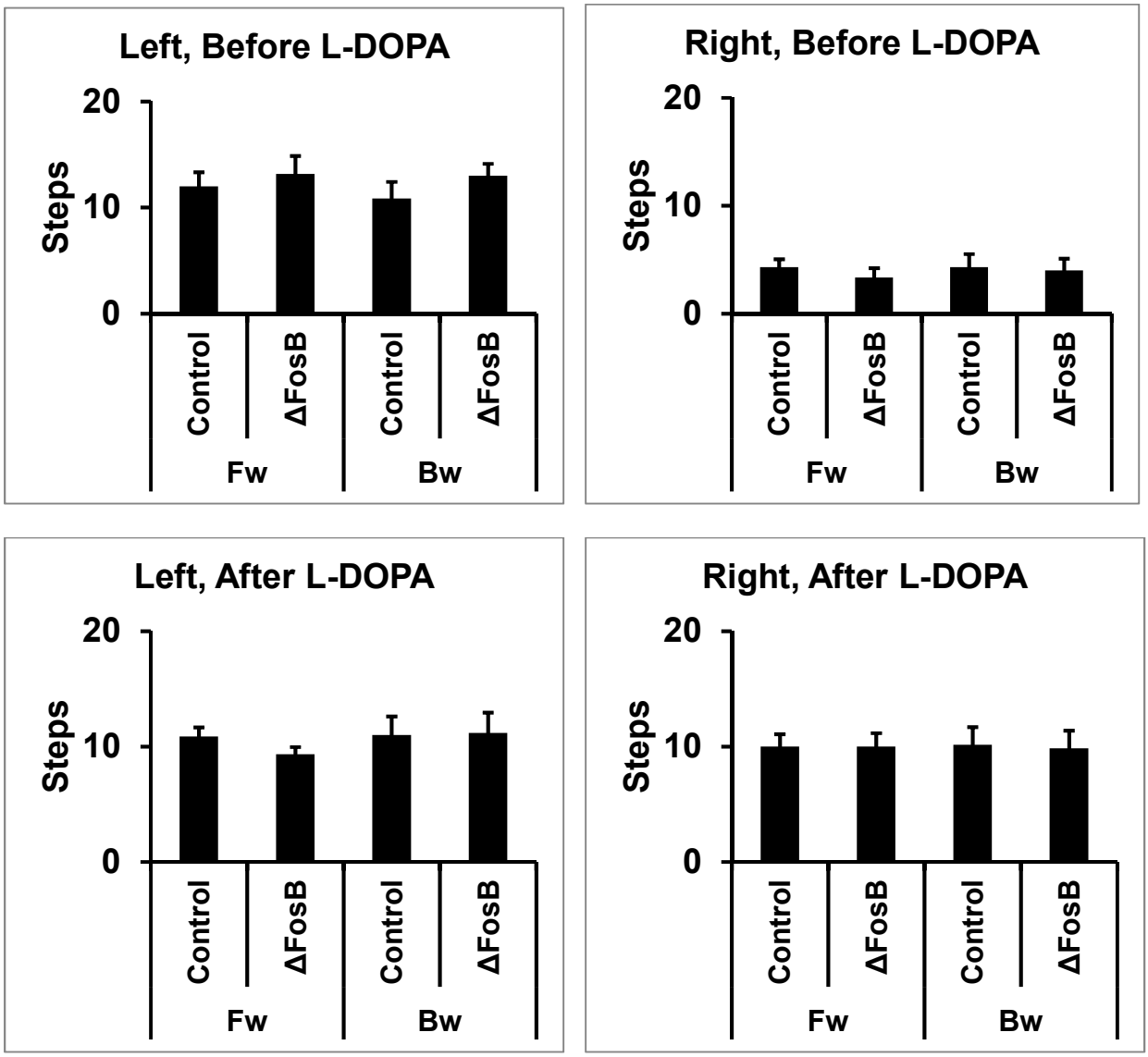

Figure 9. Before and 30 min after L-DOPA injection, there is no significant difference in adjusting steps on day 19 between the groups in either the forward or backward direction ($p > 0.05$).

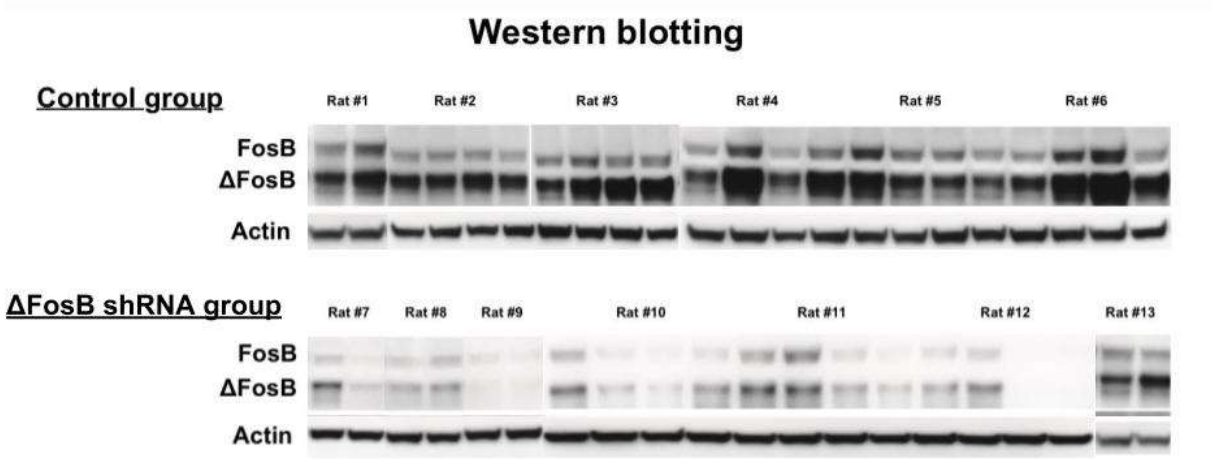

Figure 10. There is decreased ΔFosB expression in the left striatum of the rAAV-ΔFosB shRNA-GFP group, demonstrating the knockdown efficacy of the viral vector.

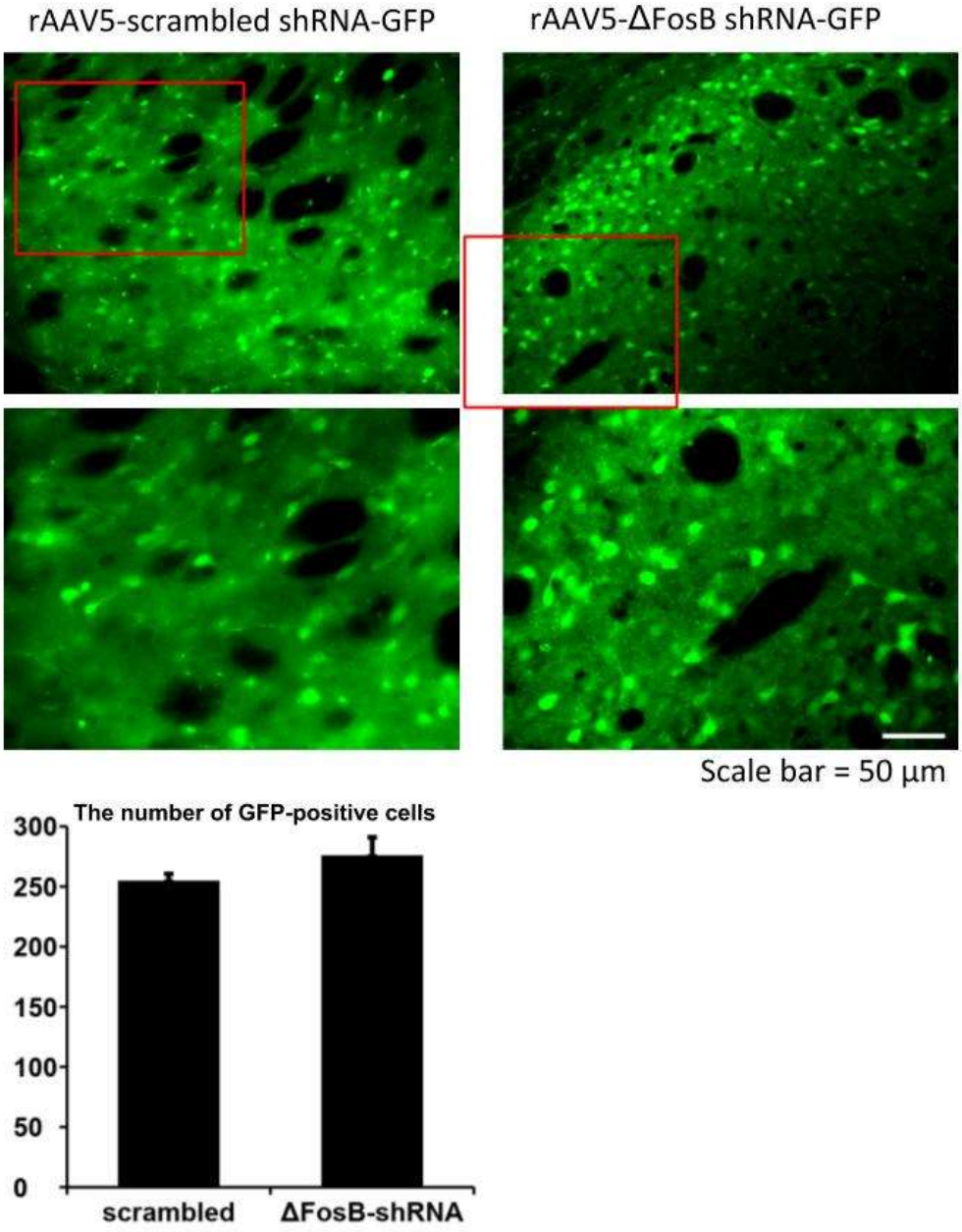

Figure 11. The IF for GFP antibody verifies the successful transduction of both viral vectors, rAAV-shRNA-GFP and rAAV- ΔFosB shRNA -GFP.

Discussion

The Western blot and AIMs scores demonstrated that the reduced expression of ΔFosB was correlative to behavioral events specific to LID (Figure 1). Therefore, as the expression decreased following the gene knockdown of ΔFosB, so did the dyskinetic behavior. At the same time, in order to address the challenges of managing LID, it was also essential that the viral vector, rAAV-ΔFosB shRNA-GFP, not diminish the effectiveness of L-DOPA's antiparkinsonian actions. The results from figures 4-9 support that claim as there was no significant difference between tests measuring extent of parkinsonism between the groups at either the beginning or end of L-DOPA treatment. Additionally, the viral vector did not lead to other behavioral changes or significant impact on health parameters during the course of testing and histological examination found no gross changes in areas injected with the virus. Taken together, the present data provide strong evidence supporting the use of viral vector-mediated gene silencing of ΔFosB to reduce LID.

These results were supported by the findings in the control group, which also underwent successful viral transduction confirmed in Figure 11, but did not show either a reduction of ΔFosB expression or AIMs. While initially both the control and ΔFosB groups had increasing AIMs scores, it is important to note that those observed in ΔFosB were always lower, though not significantly so until day 8. One possible explanation for the presence of AIMs, even on the first day of L-DOPA treatment, is that there are more factors than chronic L-DOPA treatment that contribute to the appearance of AIMs. In Putterman et al.'s experiment in hemiparkinsonian rats (2007), he and his colleagues demonstrated that subjects with high dopamine depletion in the nigrostriatal pathway, representative of PD severity, could suffer AIMs on the first day. Our

subjects, having significant dopamine depletion as a result of a 6-OHDA lesion in the medial forebrain bundle with the success of that lesion confirmed by the apomorphine test, were thus sufficiently severely parkinsonian to manifest AIMs from day one.

Therefore, it is not unreasonable that AIMs in the early days of treatment, could largely be the result of disease progression, which in practice, is generally confounded with L-DOPA treatment. In response to the repeated insult of chronic L-DOPA, the control group underwent the expected transcriptional changes that would result in AIMs, namely the upregulation of ΔFosB, which did not occur in the ΔFosB gene silencing group. Day 8 was the critical point when the two groups started to have significantly different AIMs, with AIMs becoming progressively worse in the control group, mirroring the reality of actual PD patients who develop LID. Conversely, AIMs stabilized for the ΔFosB group as the observed AIMs were primarily the consequence of the lesion. Additionally, the expression of ΔFosB in the ΔFosB gene knockdown group can be explained as the upregulation occurring from the creation of the lesion, which was made on the same day as the viral vector injection. The creation of the lesion led to elevated ΔFosB levels in the striatum because an increase in ΔFosB happens both from the transition from healthy to PD patient as well as a further increase from PD patient to advanced PD patient with LID (Tekumalla et al., 2001; Engeln et al., 2016).

During Western blot analysis, problems arose when ΔFosB expression was not visible at each of the four areas (i.e. anterior and posterior samples) for all rats. This was due to the fact that the rats were not placed in the stereotaxic frame while the brain blocks were being cut, so the process was imprecise. For some brain blocks, it was not possible to differentiate and separate anterior and posterior portions of the striatum, which then affected our results as we

were unable to obtain samples from each of these areas, with this sampling error evident in Figure 10.

In Figure 10, one illustrative example is rat thirteen, which has unusually high expression of ΔFosB within the knockdown group despite having comparable behavioral data, including AIMs scores, to other knockdown group subjects. However, rat thirteen was a subject without a sample from each area and critically, missing both its posterior samples. As the viral vector targeted the posterior part of the striatum, it may be that the virus did not readily diffuse to the anterior portion, and therefore it did not greatly alter the level of ΔFosB in those areas. We observed this in other rats, including rat twelve, finding a clear difference between the amount of ΔFosB expressed between the anterior and posterior samples.

Conclusion

Silencing ΔFosB gene expression in the striatum led to reduced AIMs without reversing the antiparkinsonian actions of L-DOPA. These results indicate the potential of gene therapy to target ΔFosB for treatment of LID in patients with advanced PD. In the future, this study along with further rodent studies will be used to guide protocols for assessment of the same viral vector strategy to knockdown ΔFosB in the NHP model. In that phase, studies will use the same viral vector, but with NHP specific sequences of shRNA to target the primate ΔFosB gene. Success of these primate experiments will validate ΔFosB's causal role in the mechanisms of LID. NHP studies may also allow further insight into whether silencing ΔFosB delays the emergence of LID, as there was no possibility to support such premise in the present study of hemiparkinsonian rats due to the rapid development of AIMs.

Beyond behavioral effects, the changes in neuronal activity in target circuits will also be examined with electrophysiologic recordings in striatum, subthalamic nucleus (STN), and globus pallidus (GP) segments. Extended behavioral and physiological studies will serve to address the global motor effects of gene silencing in PD. Other future considerations also include an evaluation of the toxicity of viral vector shRNA delivery, including inflammation and degenerative changes, which collectively will address the viability of the gene therapy as an intervention to treat LID.

Citations

1. Poewe, W. *et al*. (2017). Parkinson disease. *Nat. Rev. Dis. Primers* **3**, 17013.
2. Dorsey, E.R., Constantinescu, R., Thompson, J.P., Biglan, K.M., Holloway, R.G., Kieburtz, K., Marshall, F.J., Ravina, B.M., Schifitto, G., Siderowf, A., Tanner, C.M.
3. (2007). Projected number of people with Parkinson disease in the most populous nations, 2005 through 2030 Neurology. 68(5), 384-38. DOI: https://doi.org/10.1212/01.wnl.0000247740.47667.03
4. Klein, C., & Westenberger, A. (2012). Genetics of Parkinson's disease. *Cold Spring Harbor perspectives in medicine*, *2*(1), a008888. doi:10.1101/cshperspect.a008888
5. Schulte, C., & Gasser, T. (2011). Genetic basis of Parkinson's disease: inheritance, penetrance, and expression. *The application of clinical genetics*, *4*, 67–80. doi:10.2147/TACG.S11639
6. Poewe, W., Antonini, A., Zijlmans, J. C., Burkhard, P. R., & Vingerhoets, F. (2010). Levodopa in the treatment of Parkinson's disease: an old drug still going strong. Clin Interv Aging, 5, 229-238. 10.2147/cia.s6456
7. Thanvi, B., Lo, N., & Robinson, T. (2007). Levodopa-induced dyskinesia in Parkinson's disease: clinical features, pathogenesis, prevention and treatment. Postgrad Med J, 83(980), 384-388. doi:10.1136/pgmj.2006.054759
8. Ahlskog, J.E., & Muenter, M.D. (2001) Frequency of levodopa related dyskinesias and motor fluctuations as estimated from the cumulative literature. Mov Disord, 16(3), 448-458. doi: 10.1002/mds.1090.
9. Parkinson Study, G. (2004). Pramipexole vs Levodopa as Initial Treatment for Parkinson Disease: A 4-Year Randomized Controlled Trial. Arch Neurol. 61(7):1044–1053. doi:10.1001/archneur.61.7.1044
10. Hely, M. A., Morris, J. G. L., Reid, W. G. J., & Trafficante, R. (2005). Sydney multicenter study of Parkinson's disease: non-L-dopa-responsive problems dominate at 15 years. *Movement Disorders*. 20(2):190–199. doi: 10.1002/mds.20324.
11. Lee, C.S. Levodopa-induced dyskinesia: Mechanisms and management. BCMJ, 43(4). 206-209.
12. Manson, A., Stirpe, P., & Schrag, A. (2012). Levodopa-induced-dyskinesias clinical features, incidence, risk factors, management and impact on quality of life. J Parkinsons Dis, 2(3), 189-198. doi:10.3233/JPD-2012-120103
13. Sharma, V. D., Lyons, K. E., & Pahwa, R. (2018). Amantadine extended-release capsules for levodopa-induced dyskinesia in patients with Parkinson's disease. *Therapeutics and clinical risk management*, *14*, 665-673. doi:10.2147/TCRM.S144481\
14. Pahwa, R., Factor, S. A., Lyons, K. E., Ondo, W. G., Gronseth, G., Bronte-Stewart, H., . . . Weiner, W. J. (2006). Practice Parameter: Treatment of Parkinson disease with motor fluctuations and dyskinesia (an evidence-based review): [RETIRED]. Report of the Quality Standards Subcommittee of the American Academy of Neurology, 66(7), 983-995. doi:10.1212/01.wnl.0000215250.82576.87 %J Neurology
15. Paquette, M. A., Brudney, E. G., Putterman, D. B., Meshul, C. K., Johnson, S. W., & Berger, S. P. (2008). Sigma ligands, but not N-methyl-D-aspartate antagonists, reduce levodopa-induced dyskinesias. *Neuroreport*, *19*(1), 111–115. doi:10.1097/WNR.0b013e3282f3b0d1

16. Tekumalla, P. K., Calon, F., Rahman, Z., Birdi, S., Rajput, A. H., Hornykiewicz, O., . . . Nestler, E. J. (2001). Elevated levels of DeltaFosB and RGS9 in striatum in Parkinson's disease. *Biological Psychiatry, 50*(10), 813-816. doi:10.1016/S0006-3223(01)01234-3
17. Du, H., Nie, S., Chen, G., Ma, K., Xu, Y., Zhang, Z., . . . Cao, X. (2015). Levetiracetam Ameliorates L-DOPA-Induced Dyskinesia in Hemiparkinsonian Rats Inducing Critical Molecular Changes in the Striatum. *Parkinsons Dis, 2015*, 253878. doi:10.1155/2015/253878
18. Patterson, J. R., Kim, E. J., Goudreau, J. L., & Lookingland, K. J. (2016). FosB and ΔFosB expression in brain regions containing differentially susceptible dopamine neurons following acute neurotoxicant exposure. *Brain research, 1649*(Pt A), 53-66. doi:10.1016/j.brainres.2016.08.030
19. Cao, X., Yasuda, T., Uthayathas, S., Watts, R. L., Mouradian, M. M., Mochizuki, H., & Papa, S. M. (2010). Striatal overexpression of DeltaFosB reproduces chronic levodopa-induced involuntary movements. The Journal of neuroscience : the official journal of the Society for Neuroscience, 30(21), 7335-7343. doi:10.1523/JNEUROSCI.0252-10.2010
20. Lundblad, M., Andersson, M., Winkler, C., Kirik, D., Wierup, N., & Cenci, M. A. (2002). Pharmacological validation of behavioural measures of akinesia and dyskinesia in a rat model of Parkinson's disease. *Eur J Neurosci, 15*(1), 120-132. doi:10.1046/j.0953-816x.2001.01843.x
21. Bastide, M. F., Dovero, S., Charron, G., Porras, G., Gross, C. E., Fernagut, P.-O., & Bézard, E. (2014). Immediate-early gene expression in structures outside the basal ganglia is associated to l-DOPA-induced dyskinesia. Neurobiology of Disease, 62, 179-192. doi:https://doi.org/10.1016/j.nbd.2013.09.020
22. Berton, O., Guigoni, C., Li, Q., Bioulac, B. H., Aubert, I., Gross, C. E., . . . Bezard, E. (2009). Striatal overexpression of DeltaJunD resets L-DOPA-induced dyskinesia in a primate model of Parkinson disease. Biological Psychiatry, 66(6), 554-561. doi:10.1016/j.biopsych.2009.04.005
23. Westin, J. E., Vercammen, L., Strome, E. M., Konradi, C., & Cenci, M. A. (2007). Spatiotemporal pattern of striatal ERK1/2 phosphorylation in a rat model of L-DOPA-induced dyskinesia and the role of dopamine D1 receptors. Biological psychiatry, 62(7), 800-10. doi: 10.1016/j.biopsych.2006.11.032
24. Darmopil S., Martín A. B., De Diego I. R., Ares S., Moratalla R. (2009). Genetic inactivation of dopamine D1 but not D2 receptors inhibits L-DOPA-induced dyskinesia and histone activation. Biol. Psychiatry, 66(6), 603–613. doi: 10.1016/j.biopsych.2009.04.025.
25. Alcacer, C., Santini, E., Valjent, E., Gaven, F., Girault, J.-A., & Hervé, D. (2012). Gαolf Mutation Allows Parsing the Role of cAMP-Dependent and Extracellular Signal-Regulated Kinase-Dependent Signaling in l-3,4-Dihydroxyphenylalanine-Induced Dyskinesia. The Journal of Neuroscience, *32*(17), 5900-5910. doi:10.1523/JNEUROSCI.0837-12.2012 %J
26. Goto, S. (2017). Striatal Gα(olf)/cAMP Signal-Dependent Mechanism to Generate Levodopa-Induced Dyskinesia in Parkinson's Disease. Frontiers in cellular neuroscience, 11, 364-364. doi:10.3389/fncel.2017.00364
27. Pavón, N., Martín, A. B., Mendialdua, A., & Moratalla, R. (2006). ERK Phosphorylation and FosB Expression Are Associated with L-DOPA-Induced Dyskinesia in

Hemiparkinsonian Mice. Biological Psychiatry, 59(1), 64-74. doi:10.1016/j.biopsych.2005.05.044
28. Feyder, M., Bonito-Oliva, A., & Fisone, G. (2011). L-DOPA-Induced Dyskinesia and Abnormal Signaling in Striatal Medium Spiny Neurons: Focus on Dopamine D1 Receptor-Mediated Transmission. Frontiers in behavioral neuroscience, 5, 71. doi:10.3389/fnbeh.2011.00071
29. Valjent, E., Pascoli, V., Svenningsson, P., Paul, S., Enslen, H., Corvol, J. C., … Girault, J. A. (2005). Regulation of a protein phosphatase cascade allows convergent dopamine and glutamate signals to activate ERK in the striatum. Proceedings of the National Academy of Sciences of the United States of America, 102(2), 491–496. doi:10.1073/pnas.0408305102
30. Santini, E., Sgambato-Faure, V., Li, Q., Savasta, M., Dovero, S., Fisone, G., & Bezard, E. (2010). Distinct changes in cAMP and extracellular signal-regulated protein kinase signalling in L-DOPA-induced dyskinesia. PloS one, 5(8), e12322-e12322. doi:10.1371/journal.pone.0012322
31. Fisone, G., & Bezard, E. (2011). Molecular mechanisms of l-DOPA-induced dyskinesia. *Int Rev Neurobiol, 98*, 95-122. doi:10.1016/B978-0-12-381328-2.00004-3
32. Fiorentini, C., Savoia, P., Savoldi, D., Barbon, A., & Missale, C. (2013). Persistent activation of the D1R/Shp-2/Erk1/2 pathway in l-DOPA-induced dyskinesia in the 6-hydroxy-dopamine rat model of Parkinson's disease. Neurobiology of Disease, 54, 339-348. doi:https://doi.org/10.1016/j.nbd.2013.01.005
33. Heumann, R., Moratalla, R., Herrero, M. T., Chakrabarty, K., Drucker-Colín, R., Garcia-Montes, J. R., . . . Morelli, M. (2014). Dyskinesia in Parkinson's disease: mechanisms and current non-pharmacological interventions. 130(4), 472-489. doi:doi:10.1111/jnc.12751
34. Calabresi, P. , Di Filippo, M. , Ghiglieri, V. and Picconi, B. (2008), Molecular mechanisms underlying levodopa-induced dyskinesia. Mov. Disord., 23: S570-S579. doi:10.1002/mds.2201
35. Hope, B. T., Nye, H. E., Kelz, M. B., Self, D. W., Iadarola, M. J., Nakabeppu, Y., . . . Nestler, E. J. (1994). Induction of a long-lasting AP-1 complex composed of altered Fos-like proteins in brain by chronic cocaine and other chronic treatments. Neuron, 13(5), 1235-1244. doi:10.1016/0896-6273(94)90061-2
36. Chen, J. et al. Chronic Fos-related antigens: stable variants of deltaFosB induced in brain by chronic treatments. J Neurosci 1997;17:4933–4941. doi: 10.1523/JNEUROSCI.17-13-04933.1997
37. Hiroi, N., Marek, G. J., Brown, J. R., Ye, H., Saudou, F., Vaidya, V. A., . . . Nestler, E. J. (1998). Essential role of the fosB gene in molecular, cellular, and behavioral actions of chronic electroconvulsive seizures. J Neurosci, 18(17), 6952-6962. DOI: https://doi.org/10.1523/JNEUROSCI.18-17-06952.1998
38. Andersson, M., Westin, J. E., & Cenci, M. A. (2003). Time course of striatal DeltaFosB-like immunoreactivity and prodynorphin mRNA levels after discontinuation of chronic dopaminomimetic treatment. Eur J Neurosci, 17(3), 661-666. https://doi.org/10.1046/j.1460-9568.2003.02469.x
39. McClung, C. A., Ulery, P. G., Perrotti, L. I., Zachariou, V., Berton, O., & Nestler, E. J. (2004). ΔFosB: a molecular switch for long-term adaptation in the brain. Molecular Brain Research, 132(2), 146-154. doi:https://doi.org/10.1016/j.molbrainres.2004.05.014

40. Ulery, P. G., Rudenko, G., & Nestler, E. J. (2006). Regulation of ΔFosB Stability by Phosphorylation. *26*(19), 5131-5142. doi:10.1523/
41. Jorissen, H. J. M. M., Ulery, P. G., Henry, L., Gourneni, S., Nestler, E. J., & Rudenko, G. (2007). Dimerization and DNA-Binding Properties of the Transcription Factor ΔFosB. Biochemistry, 46(28), 8360-8372. doi:10.1021/bi700494v
42. Manczak, M., & Reddy, P. H. (2013). RNA silencing of genes involved in Alzheimer's disease enhances mitochondrial function and synaptic activity. Biochimica et biophysica acta, 1832(12), 2368–2378. doi:10.1016/j.bbadis.2013.09.008
43. Rao, D.D., Vorhies, J.S., Senzer, N., Nemunaitis, J. (2009). siRNA vs. shRNA: Similarities and differences. Adv Drug Deliv Rev,61(9):746-59. doi: 10.1016/j.addr.2009.04.004.
44. Chen, Z., Guan, Q., Cao, X., Xu, Y., Wang, L., Sun, S. J. J. o. H. U. o. S., & Technology. (2006). Effect of antisense FosB and CREB on the expression of prodynorphin gene in rats with Levodopa-induced dyskinesias. 26(5), 542-544. doi:10.1007/s11596-006-0514-7
45. Rayburn, E. R., & Zhang, R. (2008). Antisense, RNAi, and gene silencing strategies for therapy: mission possible or impossible?. *Drug discovery today*, *13*(11-12), 513–521. doi:10.1016/j.drudis.2008.03.014
46. Bartus, R. T., Weinberg, M. S., & Samulski, R. J. (2014). Parkinson's disease gene therapy: success by design meets failure by efficacy. Molecular therapy : the journal of the American Society of Gene Therapy, 22(3), 487–497. doi:10.1038/mt.2013.281
47. Paterna, J. C., Feldon, J., & Büeler, H. (2004). Transduction profiles of recombinant adeno-associated virus vectors derived from serotypes 2 and 5 in the nigrostriatal system of rats. Journal of virology, 78(13), 6808–6817. doi:10.1128/JVI.78.13.6808-6817.2004
48. Yuan, H., Sarre, S., Ebinger, G., Michotte, Y. (2005) Histological, behavioural and neurochemical evaluation of medial forebrain bundle and striatal 6-OHDA lesions as rat models of Parkinson's disease. J Neurosci Methods 144:35– 45. https://doi.org/10.1016/j.jneumeth.2004.10.004.
49. Lee, C.S., Cenci, M.A., Schulzer, M., & Bjorklund, A. (2000). Embryonic ventral mesencephalic grafts improve levodopa-induced dyskinesia in a rat model of Parkinson's disease. Brain, 123(Pt 7), 1365–1379. https://doi.org/10.1093/brain/123.7.1365
50. Cenci, M. A. and Lundblad, M. (2007), Ratings of L-DOPA-Induced Dyskinesia in the Unilateral 6-OHDA Lesion Model of Parkinson's Disease in Rats and Mice. Current Protocols in Neuroscience, 41: 9.25.1-9.25.23. doi:10.1002/0471142301.ns0925s41
51. Pandey, S., & Srivanitchapoom, P. (2017). Levodopa-induced Dyskinesia: Clinical Features, Pathophysiology, and Medical Management. *Annals of Indian Academy of Neurology*, *20*(3), 190–198. doi:10.4103/aian.AIAN_239_17
52. Mabandla, M. V., Nyoka, M., & Daniels, W. M. U. (2015). Early use of oleanolic acid provides protection against 6-hydroxydopamine induced dopamine neurodegeneration. Brain research, 1622, 64-71. doi:https://doi.org/10.1016/j.brainres.2015.06.017
53. Fang, X., Sugiyama, K., Akamine, S., & Namba, H. (2006). The stepping test and its learning process in different degrees of unilateral striatal lesions by 6-hydroxydopamine in rats. Neuroscience Research, 55(4), 403-409. doi:https://doi.org/10.1016/j.neures.2006.04.010
54. Olsson, M., Nikkhah, G., Bentlage, C., & Bjorklund, A. (1995). Forelimb akinesia in the rat Parkinson model: differential effects of dopamine agonists and nigral transplants as

assessed by a new stepping test. The Journal of Neuroscience, 15(5), 3863. DOI: https://doi.org/10.1523/JNEUROSCI.15-05-03863.1995

55. A. Berardelli, J. C. Rothwell, P. D. Thompson, M. Hallett (2001). Pathophysiology of bradykinesia in Parkinson's disease, *Brain*, 124(11), 2131–2146. https://doi.org/10.1093/brain/124.11.2131
56. Nestler, E. J., Barrot, M., & Self, D. W. (2001). DeltaFosB: a sustained molecular switch for addiction. *Proceedings of the National Academy of Sciences of the United States of America*, *98*(20), 11042-6. doi: 10.1073/pnas.191352698
57. Putterman, D.B., Munhall, A.C., Kozell, L.B., Belknap, J.K., Johnson, S.W. (2007). Evaluation of Levodopa Dose and Magnitude of Dopamine Depletion as Risk Factors for Levodopa-Induced Dyskinesia in a Rat Model of Parkinson's Disease. Journal of Pharmacology and Experimental Therapeutics. 323(1) 277-284; DOI: https://doi.org/10.1124/jpet.107.126219
58. Engeln, M., Bastide, M.F., Toulmé, E., Dehay, B., Bourdenx, M., Doudnikoff, E., Li, Q., Gross, C.E., Boué-Grabot, E., Pisani, A., Bezard, E., Fernagut, P.O., (2016). Selective Inactivation of Striatal FosB/ΔFosB-Expressing Neurons Alleviates L-Dopa-Induced Dyskinesia. *Biol* Psychiatry. 79(5) 354-361.